Experimental identification of fourth-order exchange interactions in magnets with pure spin moments

2001 J. Phys.: Condens. Matter 13 6835

(http://iopscience.iop.org/0953-8984/13/31/318)

INSTITUTE OF PHYSICS PUBLISHING JOURNAL OF PHYSICS: CONDENSED MATTER

J. Phys.: Condens. Matter **13** (2001) 6835–6852 PII: S0953-8984(01)19243-X

Experimental identification of fourth-order exchange interactions in magnets with pure spin moments

U Köbler[1], R M Mueller[1], P J Brown[2], R R Arons[1] and K Fischer[1]

[1]Institut für Festkörperforschung, FZ-Jülich, D-52425 Jülich, Germany
[2] Institut Laue-Langevin, B.P.156, F-38042 Grenoble, France

Received 21 November 2000, in final form 11 June 2001
Published 19 July 2001
Online at stacks.iop.org/JPhysCM/13/6835

Abstract

It is shown experimentally, that fourth-order exchange interactions, i.e. biquadratic, three-spin and four-spin interactions, are able to create a particular order parameter which we have called O_4. Consistently, the ordering type of O_4 always conforms to the sign of the fourth-order interaction sum evaluated from measurements of the cubic susceptibility χ_3. Earlier investigations suggest that O_4 can be identified with the expectation value of the transverse spin component, $\langle S_x \rangle$, while the conventional (Heisenberg) order parameter, O_2, is given by $\langle S_z \rangle$. Therefore, the observed ordering temperature of O_4 is never larger than the ordering temperature of O_2. The experimental signatures of O_4 are illustrated using the cubic pure spin magnets $Eu_{0.75}Sr_{0.25}Te$, GdAg, GdMg, EuS and EuO as examples. These materials provide all ferromagnetic and antiferromagnetic combinations for O_2 and O_4. For the ferromagnets EuS and EuO, second-order and fourth-order interactions are known to be ferromagnetic. This is the most complicated situation for the identification of O_4. Ac susceptibility measurements performed at different angles to an applied static magnetic field reveal the conventional rotational symmetric state around the field axis. However, measurements in the critical temperature range indicate a discontinuous rise of O_2 which is in contrast to all hitherto reported results but in agreement with mean field predictions. In most antiferromagnets in which susceptibility measurements reveal ferromagnetic O_4 the associated ordered moment is usually too small to be detected with neutron scattering without polarization analysis.

1. Introduction

This communication provides more systematic experimental evidence for the previously advanced thesis that fourth-order exchange interactions are able to generate a specific order parameter which we have called O_4 [1, 2]. The class of fourth-order exchange interactions comprises biquadratic, $\sim(S_i S_j)^2$, three-spin, $\sim(S_i S_j)(S_j S_k)$ and four-spin, $\sim(S_i S_j)(S_k S_l)$,

interactions. Evaluation of the strength of these interaction processes is possible with measurements of the cubic susceptibility $\chi_3(T)$ defined by

$$B_i = 1/\chi_1 m + 1/\chi_3 m^3 + \cdots \tag{1}$$

where B_i is the external magnetic field converted to its value inside the sample, χ_1 is the well known linear susceptibility and m is the reduced (dimensionless) magnetization [3, 4]. Assuming isotropic interactions, the two susceptibilities approach Curie–Weiss laws in the high-temperature limit (mean field approximation) with Curie–Weiss temperatures Θ_1 and Θ_3, respectively [3, 4]. This prediction was confirmed experimentally for the cubic europium chalcogenides [3]. Restricting the measurements to pure spin materials (Landé factor $g = 2$) the two experimental Curie–Weiss temperatures are given by magnetic interactions: Θ_1 is a weighted sum of second-order (Heisenberg) and fourth-order interactions while Θ_3 is given exclusively by fourth-order exchange interactions [4].

The fact that $\chi_3(T)$ also exhibits a Curie–Weiss law was interpreted as a high-temperature indication of a second ordering process exclusively due to fourth-order interactions. In the present paper we present experimental examples where this view is confirmed as correct, meaning that χ_3 diverges at the ordering temperature of O_4. It must, however, be noted that a change of sign of χ_3^{-1} usually does not correspond to an order–disorder transformation.

A very clear correlation between the sign of Θ_3 and the ordering type of O_4 was obtained recently for the diamagnetically diluted antiferromagnets $Eu_xSr_{1-x}Te$ [2, 5]. For all compositions x for which $\Theta_3 < 0$ a second antiferromagnetic phase is observed in $Eu_xSr_{1-x}Te$. This phase is distinguished by a second critical field curve with a distinguished Néel temperature. There are, so to say, two antiferromagnets in one material. We have identified this second ordering structure with O_4.

One method to distinguish between the individual fourth-order interaction processes is the analysis of the composition dependence of the Curie–Weiss temperature $\Theta_3(x)$ of the third-order susceptibility χ_3 in diamagnetically diluted samples of the magnetic material of interest [4, 6]. A comparison of the experimental $\Theta_3(x)$ and $\Theta_1(x)$ dependences in $Eu_xSr_{1-x}S$, for instance, revealed [4, 6] that the fourth-order interaction strength as given by Θ_3 is well approximated by:

$$\Theta_3(x) = -19.2x + 21.9x^2. \tag{2}$$

The coefficients in equation (2) show that biquadratic interactions are antiferromagnetic and three-spin interactions are ferromagnetic in EuS. Four-spin interactions would give a term $\sim x^3$. This term seems to be weak and could not be identified. Both coefficients in equation (2) are larger than the conventional Curie temperature of $T_C^{\parallel} = 16.5$ K for EuS. As a consequence, fourth-order interactions are strong enough to affect the spin dynamics for all temperatures: on the one hand, they are able to make the conventional order–disorder phase transition first order [7–10] and, on the other hand, they give rise to new exponents ε in the low-temperature T^{ε} Bloch law describing the deviation of the order parameter from its saturation value at absolute zero [2, 11]. The exponent ε was found to be $9/2$ for integral spin and 2 for half-integral spin in cubic pure spin materials with isotropic interactions [11]. A Bloch exponent of 2 observed for ferromagnets such as EuS, EuO and $CrBr_3$ [2, 11] is clearly at variance with present spin wave theories [12, 13].

First-order transitions caused by fourth-order exchange interactions have been predicted by numerous mean field calculations [7–10]. Our ac susceptibility measurements on EuS and EuO confirm this prediction but they also show that at this particular type of first-order transition only the order parameter is discontinuous while the linear susceptibility is well known to diverge rather normally [14–17]. Since the critical behaviour of the order parameter is extremely difficult to determine with any of the available experimental methods

the first-order character of the magnetic phase transitions has often not been recognized in the past. Moreover, very little latent heat seems to be associated with first-order transitions driven by fourth-order interactions [18, 19]. Since only the order parameter is discontinuous the macroscopic magnetic susceptibility of antiferromagnets does not necessarily exhibit a discontinuity because the susceptibility does not sample the order parameter. MnS_2 seems to be a typical example for this: although the discontinuity of the order parameter is as large as 0.66 [20] the macroscopic susceptibility gives a very weak indication only for a first-order character of the Néel transition [21]. Moreover, no hysteresis is observed [20]. Measurements of the magnetic specific heat indicate that if there is any latent heat it must be small [18]. Therefore, in cases where the discontinuity of the order parameter is much smaller, it becomes increasingly difficult to ascertain the first-order character of the magnetic phase transition. This applies in particular to neutron scattering experiments in which the critical behaviour of the order parameter is strongly masked by critical diffuse scattering intensities. Only a careful separation of both scattering contributions allows one to obtain the critical behaviour of the order parameter. In [22] more detailed investigations of the critical behaviour in the presence of fourth-order interactions are presented.

To summarize, there are a number of experimental signatures of fourth-order exchange interactions such as:

(a) Particular exponents ε in the T^{ε} Bloch law describing the deviation of the order parameter from its saturation value at absolute zero. In [11] we have illustrated how the exponent ε depends on the spin quantum number and on the dimensionality of the magnetic interactions.

(b) Deviations of the cubic susceptibility from the Curie law $\chi_3 = C_3/T$ in the high-temperature limit. In the cubic materials with pure spin magnetism considered here these deviations can be interpreted exclusively in terms of fourth-order exchange interactions and/or correlations [4]. In particular, in insulators a Curie–Weiss law is observed for χ_3. This makes χ_3 a very valuable quantity for a quantitative investigation of fourth-order interactions.

(c) Observation of a second ordering process which has all characteristics of an order–disorder phase transition although it occurs in an ordered state. This conforms qualitatively to predictions made by mean field calculations including fourth-order interactions: there is first an order–disorder phase transition with a possible but not necessarily discontinuous rise in magnetization into a collinearly ordered spin phase. At some lower temperature a transition into a canted spin phase occurs [10]. Although these predictions seem to be physically relevant our experiments show that it is not appropriate to view the second transition as a spin reorientation process or an order–order phase transition because the already existing order parameter O_2 exhibits no anomaly at this second phase transition [1]. This shows the orthogonality of both ordering structures and justifies the definition of an independent order parameter O_4.

(d) Although there are different reasons for magnetic first-order transitions, fourth-order interactions frequently lead to a first-order transition in the sense that only the order parameter is discontinuous [7–10].

Here we focus on the experimental identification of O_4. We restrict ourselves to a few selected materials for which all antiferromagnetic and ferromagnetic combinations occur for O_2 and O_4. The most intriguing situation is given if O_2 and O_4 are ferromagnetic. This can be expected for EuS and EuO, since $\Theta_1 > 0$ and $\Theta_3 > 0$ for both materials [3]. A geometrical distinction between the two assumed order parameters by means of a magnetic field is therefore not possible because neither of them will be aligned parallel to the field. Since the resulting

magnetic state is expected to be non-collinear, we performed ac susceptibility measurements transverse to an applied static magnetic field. In principle, these measurements are more suitable for the detection of small deviations from a collinear spin structure than longitudinal measurements. However, they have to be carried out on highly perfect spherical samples. For sample shapes deviating from a rotational symmetric ellipsoid the demagnetization field is not precisely defined. As a consequence, a state with a non-uniform magnetization due to magnetic domains with moment components transverse to the field persists up to the largest applied fields.

Our experiments on EuO and EuS single-crystal spheres reveal no anomalous behaviour of the transverse susceptibility. The observation of the conventional rotational symmetric magnetic state around the field axis, however, does not definitely exclude our assumption of a non-collinear magnetic state. It only shows that the vectorial sum of all transverse moment components is zero.

2. Experimental details

For a number of insulating magnetic materials a quantitative measure for the fourth-order interaction sum is now available by the experimental Curie–Weiss temperature Θ_3 of the third-order susceptibility χ_3 [2, 3]. In metals, no Curie–Weiss law is observed for χ_3 [1, 23, 24]. Instead, χ_3 shows a strong temperature dependence only near its divergence at the ordering transition of O_4 but assumes a very weak temperature dependence for high temperatures. This implies that the sign of the fourth-order interaction sum can change as a function of temperature in metals. Even the sign of χ_3^{-1} can change as a function of temperature [23], which formally corresponds to a divergence but without indicating a phase transition. Strength and type (i.e. sign) of the total fourth-order interaction must in those cases be estimated from the difference between the experimental χ_3 value and the calculated Curie value for χ_3, assuming $\Theta_3 \equiv 0$. Table 1 compiles for a number of Eu and Gd compounds the established ordering types of O_2 and the predicted ordering types for O_4 according to neutron scattering and magnetization studies, preferentially measurements of χ_3.

Table 1. Established ordering types of conventional order parameter O_2 and proposed ordering types for O_4.

	EuO	EuS	GdS	$Gd_{0.8}Eu_{0.2}S$	GdMg	EuTe	$Eu_{0.75}Sr_{0.25}Te$	GdAg
O_2	ferro	ferro	anti	anti	ferro	anti	anti	anti
O_4	ferro	ferro	ferro	anti	anti	ferro	anti	ferro

We start by discussing one material with both order parameters antiferromagnetic. This is the most convenient situation since the order parameters are easily distinguished on account of their different critical fields $B_c(T)$ which are marked by clear anomalies in conventional, i.e. field-parallel, magnetization curves. The extrapolations $B_c \to 0$ for both $B_c(T)$ curves give the two Néel temperatures.

Table 1 contains two such examples. Since $Gd_{0.8}Eu_{0.2}S$ was discussed in detail in [23] we focus here on $Eu_{0.75}Sr_{0.25}Te$. For the diamagnetically diluted antiferromagnets $Eu_xSr_{1-x}Te$ it was shown [2, 3, 25] that antiferromagnetic biquadratic interactions dominate over ferromagnetic three-spin interactions for $x < 0.85$ such that $\Theta_3 < 0$ for $x < 0.85$. Hence, both order parameters are antiferromagnetic for $x < 0.85$ in $Eu_xSr_{1-x}Te$. This can be proved by the observation of two different critical field curves. Figure 1(a) presents a differentiated low-temperature magnetization curve of $Eu_{0.75}Sr_{0.25}S$, revealing one narrow

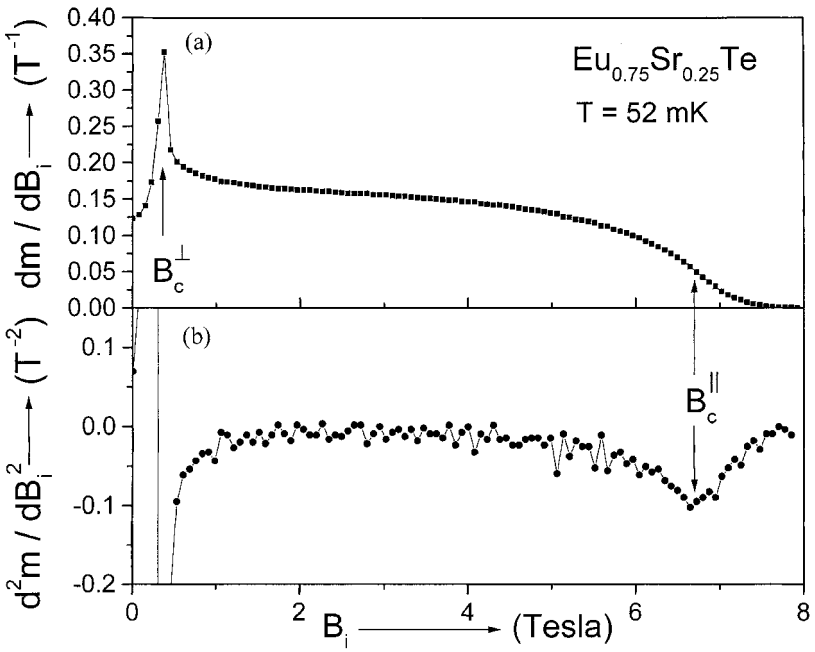

Figure 1. (a) First derivative $\mathrm{d}m/\mathrm{d}B_i$ of normalized magnetization m versus internal field B_i for $Eu_{0.75}Sr_{0.25}Te$ at a temperature of 52 mK. The inflection point at $B_c^{\parallel}$ is identified as the critical field of conventional order parameter O_2 and the peak at $B_c^{\perp}$ is the critical field of transverse order parameter O_4. (b) Second derivative of normalized magnetization allowing a more precise localization of the critical field $B_c^{\parallel}$.

maximum at $B_c^{\perp} \sim 0.35$ T and a second anomaly at $B_c^{\parallel} \sim 6.7$ T where an inflection point is noticed. This anomaly is seen more clearly as an extremum in the second derivative of magnetization as is shown in figure 1(b). Since both anomalies also give rise to magnetocaloric effects [25] one can be sure that we are dealing with phase transitions. It should be noted that the phase transition at $B_c^{\perp}$ is absent for the $Eu_xSr_{1-x}Te$ samples with $x > 0.85$, for which O_4 is assumed to be ferromagnetic because $\Theta_3 > 0$ [25].

Performing magnetization measurements such as in figure 1 for different temperatures as well as magnetization measurements as a function of temperature for different fields the complete $B_c^{\perp}(T)$ and $B_c^{\parallel}(T)$ curves can be obtained. These are shown in figure 2 for a sample of composition $Eu_{0.7}Sr_{0.3}Te$. Note the much smaller $B_c^{\perp}$ values compared to the $B_c^{\parallel}$ values. Apparently, O_4 is much less stable against the application of a magnetic field than O_2. The two very similar Néel temperatures confirm that the fourth-order interactions are approximately as strong as the second-order interactions. It must be considered as characteristic that no definite anomaly can be seen in the $B_c^{\parallel}(T)$ curve at $T_N^{\perp}$. This is in accordance with the assumed orthogonality of both ordering structures.

We can give only a very approximate value for the ordered saturation moment of O_4. Since both order parameters give rise to the same set of half-integral neutron scattering lines of the MnO type [5, 25] it is not possible to distinguish them in zero field neutron scattering experiments. On measuring the low-temperature scattering intensities as a function of field, a sudden intensity decrease is observed at $B_c^{\perp}$ with increasing field [5]. This intensity loss corresponds to the disappearance of O_4 at the critical field $B_c^{\perp}$. In [5]

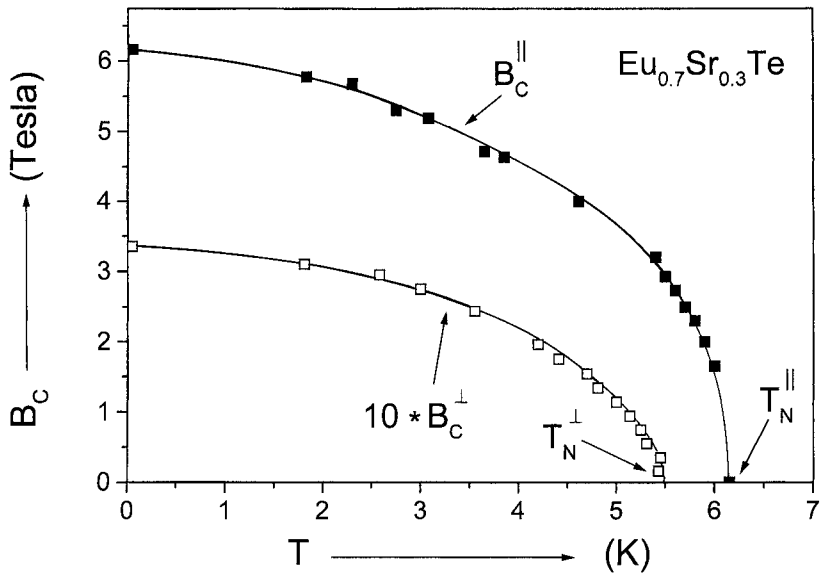

Figure 2. Critical fields $B_c^{\parallel}$ and $B_c^{\perp}$ of $Eu_{0.7}Sr_{0.3}Te$ as a function of temperature. The two similar Néel temperatures show that second-order and fourth-order exchange interactions have a comparable strength. Note, however, that $B_c^{\perp}$ values are smaller by a factor of 20 compared to $B_c^{\parallel}$ values. Full curves are guides to the eye only. No definite anomaly is visible in the $B_c^{\parallel}(T)$ curve at $T_N^{\perp}$.

a proportion of $O_4/O_2 \sim 0.4$ was estimated. This means that the saturation moment of O_4 is about 2.6 μ_B. Alternatively, in macroscopic magnetization measurements [2] one would rather estimate a saturation value ~ 1 μ_B from the observed magnetization increase at $B_c^{\perp}$. This is a frequently observed discrepancy: neutron scattering shows larger magnetization changes than macroscopic measurements of the field parallel magnetization component.

We now turn to GdAg as an example for the combination O_2 = antiferromagnetic and O_4 = ferromagnetic. For this class of magnets the Curie temperature of O_4 is marked by a sudden strong field dependence of the magnetic susceptibility. This has been observed for the antiferromagnets EuTe [2], GdS [23] and GdAg [24]. While for EuTe and GdS the susceptibility becomes field dependent just at the Néel temperature indicating that the Néel temperature of O_2 and the Curie temperature of O_4 are identical, the two ordering temperatures are clearly different for GdAg for which $T_N^{\parallel} = 134$ K and $T_C^{\perp} \approx 100$ K. Figure 3 shows conventional dc susceptibility measurements on a polycrystalline GdAg sample obtained for different values of the applied magnetic field. At the conventional Néel temperature of $T_N^{\parallel} = 134$ K only a weak maximum can be seen. For an ideal isotropic antiferromagnet we would expect that the susceptibility decreases to $\chi(T = 0) = 2/3 * \chi(T_N^{\parallel})$ due to an isotropic distribution of magnetic domains. Instead, the susceptibility of GdAg decreases much more weakly for $T < T_N^{\parallel}$ and becomes strongly field dependent at about 100 K. This temperature we identify as the Curie temperature $T_C^{\perp}$ of O_4. Evidence for this is provided by the divergence of the cubic susceptibility χ_3 at $T_C^{\perp} \approx 100$ K. Figure 3 also shows that for fields smaller than 10 mT, field cooled (FC) and non-field cooled (NFC) susceptibility curves typically have different characteristics below $T_C^{\perp}$. The lack of thermodynamic equilibrium below $T_C^{\perp}$ also confirms that we are dealing with a particularly long-range magnetic order.

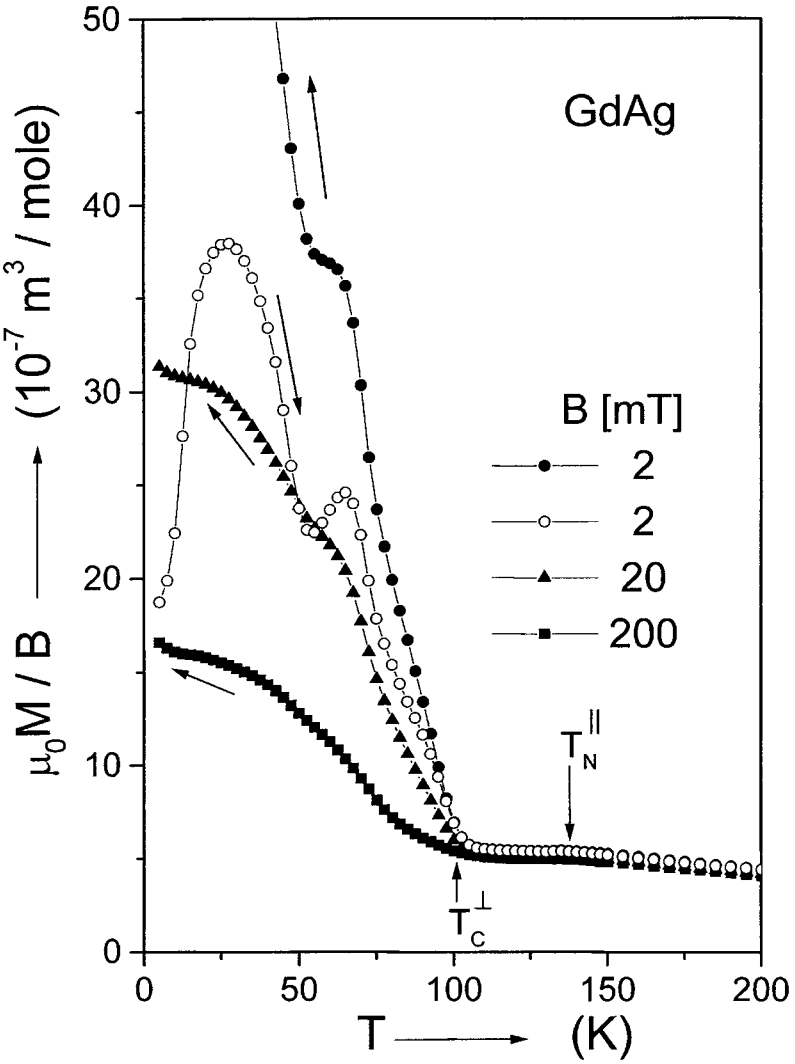

Figure 3. Static susceptibility of a polycrystalline GdAg sample measured in different external magnetic fields B_o. The temperature $T_C^{\perp}$ at which a sudden strong field dependence sets in is identified as the Curie temperature of O_4. For fields $B_o < 10$ mT hysteresis is observed for $T \leqslant T_C^{\perp}$ as is typical for an ordered state. At the conventional Néel temperature $T_N^{\parallel}$ only a weak maximum can be seen.

To show the divergence of χ_3 at $T_C^{\perp}$, magnetic isotherms have to be measured up to the largest available field in order that their small curvature can clearly be detected. Note that χ_3 describes the curvature of the magnetic isotherms according to equation (1). For an ideal isotropic antiferromagnet with no fourth-order interactions a linear relation between the low-temperature magnetization and the magnetic field is expected. This can easily be shown theoretically and was borne out also by computer simulations for EuTe [26]. For such an antiferromagnet, Θ_3=0 and χ_3 obeys the Curie law $\chi_3 = C_3/T$ in the high-temperature limit. At T_N, χ_3 diverges meaning that the magnetization becomes a linear function of the field (see equation (1)). For all temperatures $T \leqslant T_N$, χ_3 remains infinite, i.e. the magnetization

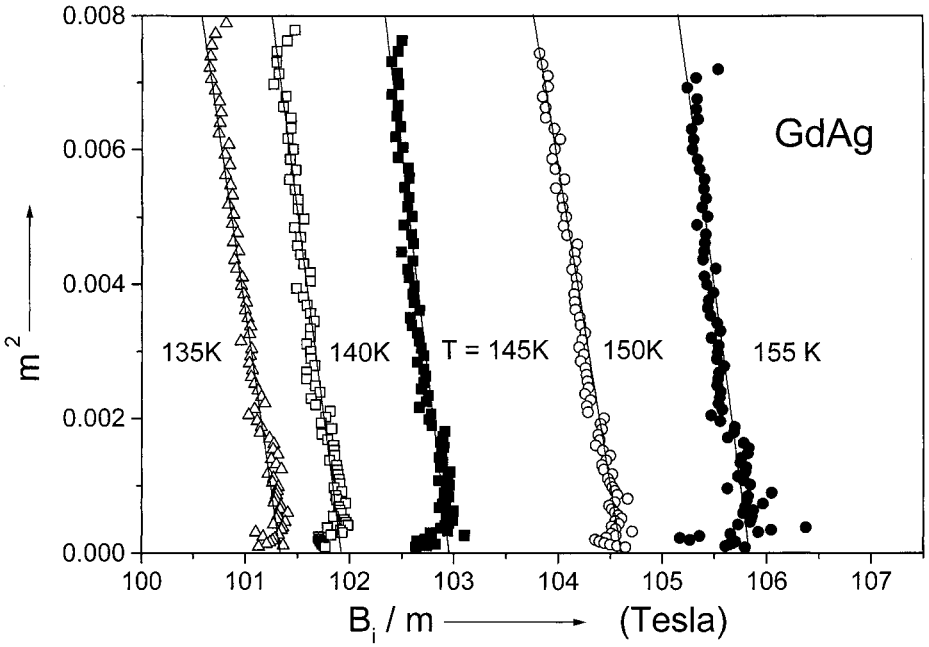

Figure 4. Paramagnetic isotherms of GdAg plotted as squared reduced magnetization m^2 versus B_i/m (Arrott plot). The slopes of these lines give the cubic susceptibility χ_3 which is negative, meaning that the magnetization increases faster than linearly with field. Fourth-order interactions are therefore ferromagnetic.

increases linearly with field[1]. Unfortunately, there is no isotropic antiferrromagnet known to us which would show these properties.

Magnetization curves of GdAg are anomalous in that they increase faster than linearly with field for all temperatures. This corresponds to a negative cubic susceptibility. In contrast to the insulating antiferromagnet EuTe [2, 3] the cubic susceptibility of the metallic antiferromagnets GdAg and GdS [23] does not approach the anticipated Curie–Weiss law in the high-temperature limit. This does not fit the mean field model, but the negative cubic susceptibility is characteristic for ferromagnetic fourth-order interactions and therefore consistent with the observed ferromagnetic O_4 in GdAg. In figure 4 we show a selection of paramagnetic isotherms for GdAg plotted as squared reduced magnetization m^2 versus B_i/m (Arrott plot). It can be seen that the cubic susceptibility, i.e. the slope of the isotherms, is negative even in the paramagnetic phase. Due to the strong antiferromagnetic bilinear interactions (i.e. the large Néel temperature), reduced magnetization values of less than 0.1 are reached in the available field of 8 T. It is therefore difficult to obtain accurate χ_3 values from the weak observed curvature of the isotherms. Note that the reciprocal linear susceptibility B_i/m changes by only 0.5% between zero field (lower end of isotherm) and 8 T (upper end of isotherm).

Figure 5 displays the temperature dependence of the reciprocal cubic susceptibility as obtained from the slopes in Arrott plots like in figure 4. It becomes apparent from figure 5(a) that χ_3 diverges with the mean field exponent of unity at $T_C^{\perp} \approx 100$ K, but in contrast to the mean field model the amplitude is negative. The same situation was observed for GdS, but

[1] This can be considered a degeneracy which can be lifted by the fourth-order interactions.

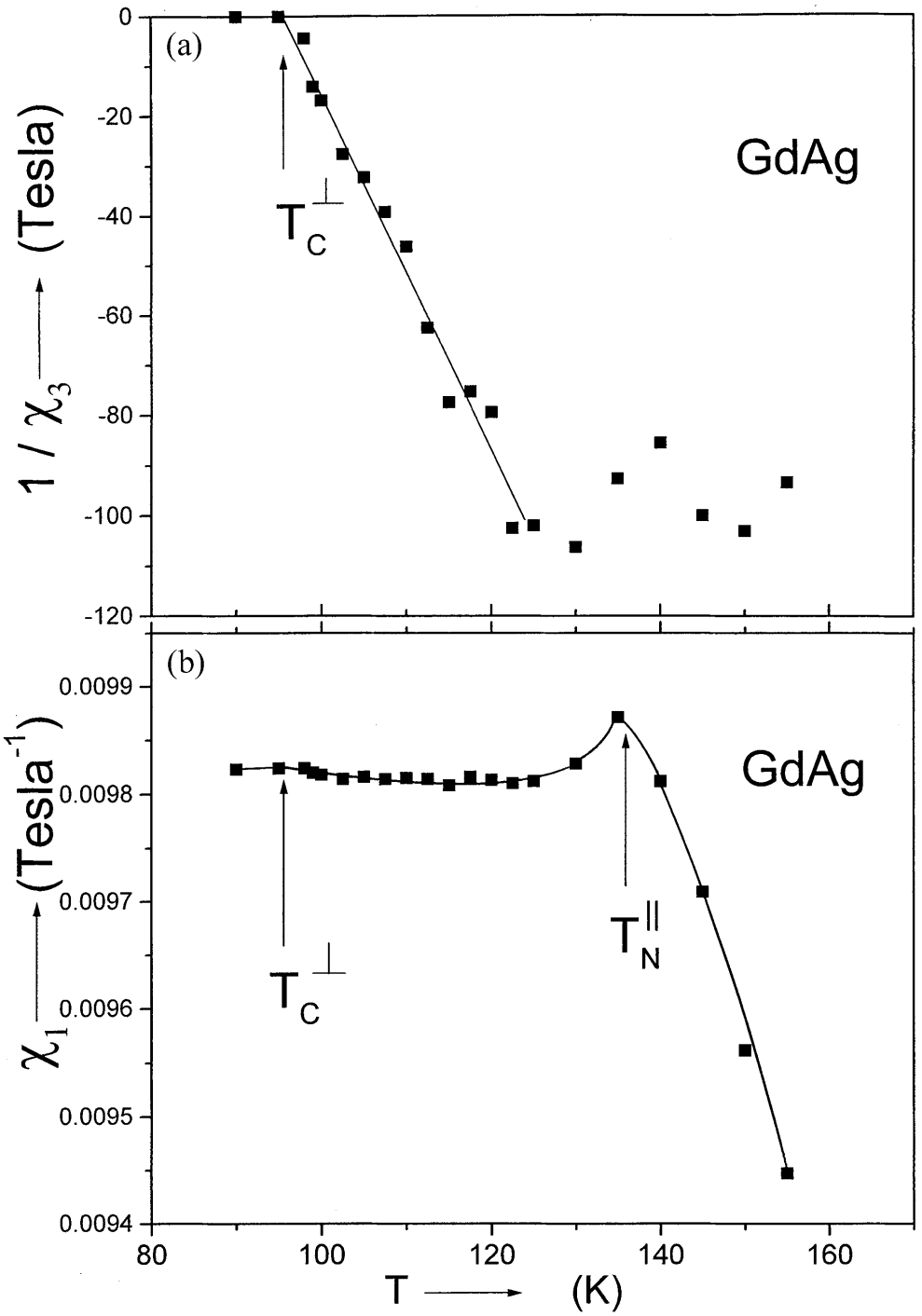

Figure 5. (a) Inverse cubic susceptibility χ_3^{-1} of GdAg as a function of temperature. χ_3 is negative and diverges with mean field critical exponent of unity at $T_C^{\perp} \approx 100$ K. (b) Linear susceptibility χ_1 as a function of temperature. These data have been obtained from the intersections of the magnetic isotherms in the Arrott plot with the abscissa (see figure 4). Note the strongly suppressed zero point in comparison with figure 3.

there $T_N^{\parallel}$ and $T_C^{\perp}$ are identical [23]. In figure 5(b) the high-field linear susceptibility χ_1 obtained from linear extrapolations $m^2 \to 0$ in the Arrott plot (figure 4) are seen in a representation with a strongly suppressed zero point. In this graph the Néel temperature $T_N^{\parallel}$ is seen somewhat clearer than in figure 3, but in contrast to figure 3 no pronounced anomaly can be noticed at the Curie temperature $T_C^{\perp}$ in figure 5(b). This is because the strong field dependence of the susceptibility seen in figure 3 is limited to small field values for which the antiferromagnetic domains rotate such that, finally, the moments are oriented nearly perpendicular to the field. For $T < T_C^{\perp}$ the magnetic isotherms become more and more curved in the Arrott plot and a meaningful evaluation of χ_1 and χ_3 is no longer possible.

The fact that in GdAg χ_3 diverges at 100 K verifies that we are dealing with an intrinsic Curie-type transition induced by fourth-order interactions and not with a ferromagnetic precipitation or some contamination of the sample as it was assumed in [24]. Moreover, the Gd–Ag phase diagram contains no other phase near to the 1:1 composition [27]. Our conclusion is further supported by specific heat measurements which reveal a small anomaly at $\approx$100 K [28]. From low-temperature magnetization curves it can be estimated that the ordered saturation moment of O_4 is only about 0.1 μ_B. This value is too small to be detected with neutron scattering without polarization analysis, but it conforms to the spontaneous magnetic moment observed in weak ferromagnets such as NiF_2 (0.03 μ_B) having a tetragonal crystal structure [29]. The fact that in contrast to NiF_2 there is no finite resulting spontaneous magnetization in GdAg we ascribe to a particular domain structure whereby the spontaneous moments compensate. These domains are not free to rotate as revealed by the thermodynamic non-equilibrium observed for $T \leqslant T_C^{\perp}$.

Next we discuss GdMg as the best example for the situation O_2 = ferromagnetic and O_4 = antiferromagnetic [1, 30, 31]. In this case the ferromagnetic component due to O_2 can be aligned parallel to a magnetic field. Indirect evidence for antiferromagnetic O_4 is given by a reduced longitudinal spontaneous magnetization. Ac susceptibility measurements perpendicular to the field allow a direct identification of antiferromagnetic O_4 and its transition temperature $T_N^{\perp}$ because they contain no signal from O_2 and $T_C^{\parallel}$ [1]. GdMg is exceptional in that the ordered magnetic moment of O_4 is as large as $\sim$5 μ_B [31]. Therefore, no intensity problems occur in detecting this component with neutron scattering. Extremely large fields are necessary to force the antiferromagnetic component into the field direction [30–32].

If the two order parameters are different in type as applies for GdMg they give rise to different sets of magnetic scattering lines and can thus easily be distinguished, apart from possible intensity problems if the ordered moment of O_4 is weak. In GdMg, ferromagnetic O_2 contributes to the scattering lines with integral indices while antiferromagnetic O_4 gives rise to scattering lines with half-integral indices. In figure 6 we present examples for the temperature dependence of the integrated scattering intensities of the two types of lines. These data have been obtained on instrument D9 at the hot neutron source of ILL in Grenoble using a wavelength of $\sim$0.463 Å. Figure 6 displays the normalized diffraction intensities I_{HKL}/I_{HKL} $(T = 0)$ of the ferromagnetic 0, 0, 3 Bragg line (after subtraction of a small nuclear contribution) and of the antiferromagnetic 0, 0, 3/2 Bragg line. Both order parameters exhibit a T^2 law at low temperatures. This law has been fitted to the intensity data in figure 6. It can be seen that the phase transition at $T_N^{\perp}$ is preceded, like the phase transition at $T_C^{\parallel}$, by critical diffuse scattering intensities and has therefore the characteristics of an order–disorder phase transition. Note that at $T_N^{\perp}$ no anomaly is visible in the 0, 0, 3 intensity curve. This is in keeping with the mutual orthogonality of both ordering structures [31]. Due to their different critical temperatures and their comparable strengths, both phase transitions are well resolved in specific heat measurements [1, 33].

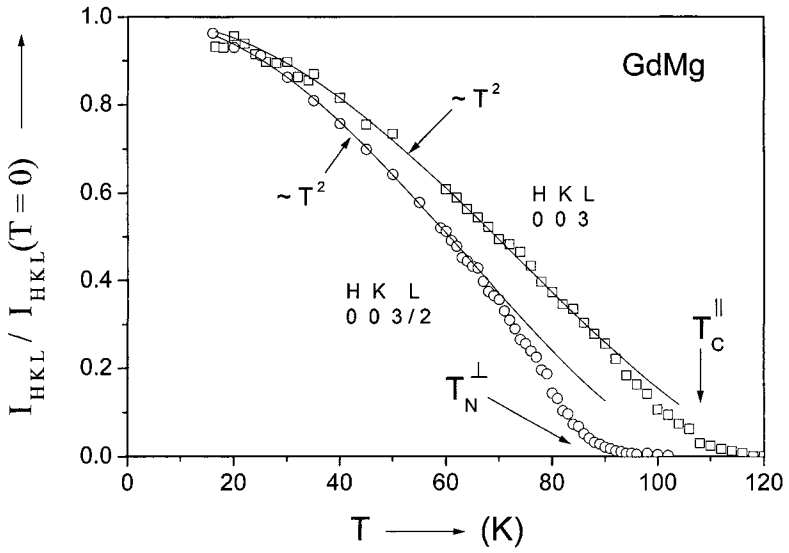

Figure 6. Normalized integrated neutron scattering intensities I_{HKL}/I_{HKL} $(T = 0)$ of GdMg for the ferromagnetic 0, 0, 3 diffraction line and the antiferromagnetic 0, 0, 3/2 diffraction line as a function of temperature. Note that virtually no anomaly is seen in the 0, 0, 3 intensity curve at $T_N^{\perp}$. For both types of line the T^2 law for the order parameter has been fitted.

We now turn to EuS and EuO as examples for the intriguing situation in which O_2 and O_4 can be expected to be ferromagnetic. A further example of this class of materials seems to be GdZn [24]. The fourth-order interaction sum as given by Θ_3 was evaluated as $\Theta_3 = +2.0$ K for EuS and $\Theta_3 = +12$ K for EuO [3]. The two anticipated ferromagnetic order parameters give rise to the same set of magnetic Bragg lines with integral indices. Therefore, in zero field neutron scattering experiments, i.e. in the presence of magnetic domains, it is not possible to distinguish the two ordering structures. Because an orthogonal configuration of magnetization components can be expected we must consider that neither component can be aligned perfectly parallel to a magnetic field. A simple geometrical distinction between them is therefore not possible.

In order to search for deviations from a nearly ferromagnetic but non-collinear spin arrangement, measurements transverse to a static magnetic field are better suited than measurements parallel to the field. We performed ac susceptibility measurements for different angles Φ between the static magnetic field B_o and the axis of the ac measuring system. The ac frequency was 27 Hz and the amplitude $B_{\approx}$ of the excitation field was less than 10^{-4} T. It is very important to use perfectly ground spherical samples in this experiment. For any sample shape deviating from a rotationally symmetric ellipsoid, an infinite magnetic field is necessary to rotate all magnetic domains into the field direction.

Figure 7 shows a selection of χ measurements on an EuO single crystal sphere for different angles Φ. These data have been obtained at a temperature of 4.2 K which is small compared to the Curie temperature of 69.2 K. Below the demagnetization field of $B_D = 0.8$ T all susceptibilities are identical and given by the reciprocal demagnetization factor $N^{-1} = 3$. Note that we make use of the dimensionless susceptibility defined as $\chi = J/B$ with the magnetic induction of the sample, J, and the magnetic field, B, both given in Tesla.

In the limit $T \to 0$ the susceptibility $\chi^{\parallel}$ parallel to the static field B_o should suddenly drop to zero at B_D. This is not quite the case. A closer look at the steep flank near B_D shows that

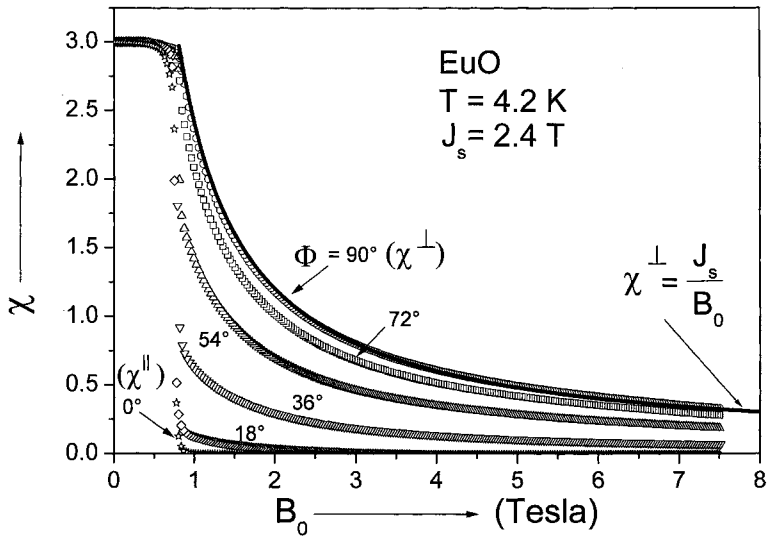

Figure 7. Ac susceptibilities for an EuO single-crystal sphere measured at an angle Φ to a static magnetic field B_o as a function of B_o. The susceptibility perpendicular to B_o, χ^{-1}, can be described by $\chi^{-1} = J_s/B_o$ with $J_s = 2.4$ T as the saturation magnetic density of EuO (full curve).

the decrease $\chi^{\parallel} \rightarrow 0$ is continuous. Measurements at 100 mK, i.e. in the thermodynamically saturated state, using an increased number of data points per field unit confirm the continuous behaviour of $\chi^{\parallel}$ at B_D. This makes the evaluation of the spontaneous magnetization a rather undefined task and necessitates some extrapolation procedure. However, the $\chi^{\parallel}$ data rapidly fall below values of the order of 10^{-3} for $B_o > B_D$. The longitudinal (field parallel) susceptibility therefore seems to saturate in a rather normal way apart from the range close to B_D.

To show this more clearly, we have integrated the $\chi^{\parallel}(B_o)$ data to visualize the nearly perfect saturating behaviour of the field-parallel magnetization component of EuO. As can be seen from figure 8 the deviations from saturation are very small and correspond to the thermodynamically not quite saturated state at 4.2 K. As we know from ^{153}Eu NMR measurements [11] the thermal decrease of the normalized spontaneous magnetization of EuO is given with a high precision by $m = 1 - 1.05 \times 10^{-4}T^2$. Inserting $T = 4.2$ K gives $m = 0.998$ which conforms quite well to the observed magnetization values at $B_D = 0.8$ T in figure 8. The still remaining deviations from saturation at 100 mK are too small to justify a quantitative interpretation in terms of an intrinsic effect.

Also the transverse ac susceptibility $\chi^{\perp}$ conforms to what can be expected if the magnetization is aligned by a static magnetic field B_o. The full curve in figure 7 is calculated according to the simple expression $\chi^{\perp} = J_S/B_o$ with $J_s = 2.4$ T as the theoretical saturation magnetic density (induction) of EuO. It can be seen that this function fits the experimental $\chi^{\perp}$ data rather perfectly and that the transverse susceptibility is very large even for strong longitudinal fields.

Since we are interested in the behaviour of the magnetization in an external field $B_o > B_D$ we need not consider demagnetization effects in the analytical expression of the transverse ac susceptibility. To show this explicitly we assume that the magnetization is always parallel to the resulting magnetic field which is given by the vectorial sum of the longitudinal static field B_o and the perpendicular ac field $B_{\approx}$. We then have:

$$\chi^{\perp} = J^{\perp}/B_{\approx} = J^{\parallel}/B_o = [(J_s)^2 - (J^{\perp})^2]^{0.5}/B_o \tag{3}$$

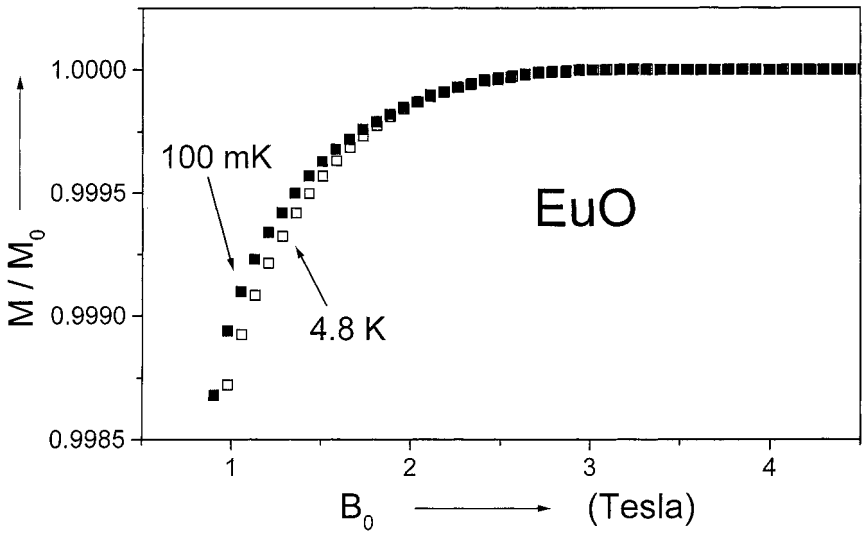

Figure 8. Normalized field parallel magnetization of an EuO single-crystal sphere as a function of external field B_o for temperatures of 100 mK and 4.8 K. In high fields a nearly ideal saturating behaviour is observed.

since $J_s^2 = (J^{\parallel})^2 + (J^{\perp})^2$. Re-writing the extreme left and right sides of equation (3) we obtain for the squared expressions:

$$(\chi^{\perp})^2 (B_o)^2 = (J_s)^2 - (\chi^{\perp})^2 (B_{\approx})^2. \tag{4}$$

We now normalize the perpendicular susceptibility by requesting that $\chi^{\perp} = 3$ at $B_o = B_D = 0.8$ T. This gives the relation:

$$9(B_D)^2 = (J_s)^2 - 9(B_{\approx})^2. \tag{5}$$

Equation (5) can be used to eliminate $B_{\approx}$ in equation (4). Considering that $B_D = 1/3 * J_s$ we obtain

$$\chi^{\perp} = J_s / B_o \tag{6}$$

with $J_s = 2.4$ T for EuO and 1.5 T for EuS. Practically, equation (6) results immediately from equation (4) considering that $B_{\approx}$ is of the order of 10^{-4} T but B_o and J_s are of the order of 1 T.

Reading the $\chi(\Phi)$ data at a constant external field B_o results into the quite normal dependence $\chi(\Phi) \sim \sin^2(\Phi)$. As a conclusion, the ac susceptibility confirms the rotational symmetric state around the field axis as is expected for a classical magnetization vector aligned by a static magnetic field. This does not, however, exclude our assumption of a non-collinear magnetic structure but it shows that the vectorial sum of all moments adds to the expected total moment, i.e. the vectorial sum of all transverse moments is zero.

In many materials it is observed that the critical temperatures of O_2 and O_4 are very similar (see figure 2) or even identical as applies for EuTe [2] and GdS [23]. We therefore investigated the critical temperature range of EuS and EuO in more detail using ac susceptibility measurements on our spherical single crystals. If the magnetization changes very rapidly as a function of field and temperature as is the case in the critical range, ac measurements are better suited than dc measurement.

In figure 9 we present a selection of ac susceptibility curves $\chi^{\perp}$ for an EuS sphere obtained for fields smaller than the demagnetization field of $B_D(T \to 0) = 0.5$ T. These curves have

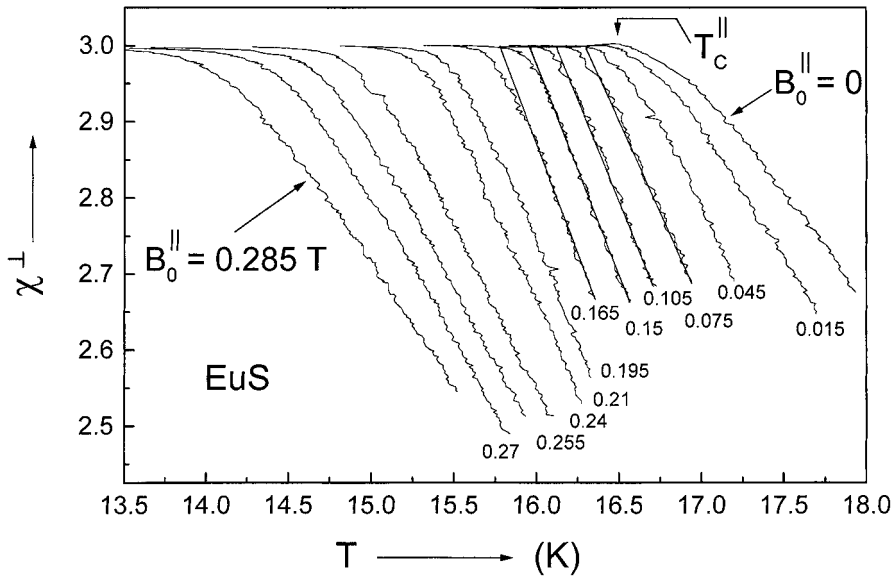

Figure 9. Ac susceptibility curves $\chi^{\perp}(T)$ for the indicated longitudinal magnetic fields measured on an EuS single-crystal sphere perpendicular to the field. The level $\chi^{-1} = 3$ marks an internal field of zero. The extrapolation $\chi^{\perp} \to 3$ gives the demagnetization field $B_D(T)$ which is proportional to the spontaneous polarization $J_{sp} = 3B_D$. For details see text.

been measured transverse to the static magnetic field but this is of no importance for the extrapolation $B_i \to 0$. By close examination of these curves one can distinguish three groups with a qualitatively different behaviour. For fields $B_o < 0.05$ T the ac susceptibility curves exhibit a pronounced concave up curvature and all reach the demagnetization plateau of $\chi = 3$ at nearly the same temperature. This point unambiguously marks the Curie temperature.

The next group of curves for field values of $0.05 < B_o < 0.17$ T are fairly parallel and exhibit only moderate rounding near the demagnetization plateau $\chi = 3$. For fields $B_o > 0.17$ T the ac susceptibility curves become consecutively more inclined to the left-hand side and deflect increasingly to smaller temperatures instead of reaching the plateau of $\chi = 3$.

The spontaneous magnetization J_{sp} is obtained from the demagnetization field B_D according to $J_{sp}(T) = 3B_D(T)$. $B_D(T)$ is defined for $B_i \to 0$, i.e. by the kink temperature at $\chi = 3$. Since all $\chi(T)$ curves are more or less rounded near $\chi = 3$ it is necessary to obtain the kink temperature by extrapolation. This procedure introduces considerable ambiguities in all macroscopic evaluations of the spontaneous magnetization. Moreover, for EuS a meaningful linear extrapolation is possible only for the $\chi(T)$ curves with $0.05 < B_o < 0.17$ T. This procedure is indicated by straight lines in figure 9. Clearly, a linear extrapolation is not possible for the rounded curves with $B_o < 0.05$ T which reach the $\chi = 3$ level at nearly the same temperature. A linear extrapolation again becomes more and more questionable for the high-field susceptibility curves on the left-hand side of figure 9, such that the meaning of the as-obtained spontaneous magnetization values becomes unclear.

In figure 10 we present the spontaneous magnetization curve for EuS obtained using the extrapolation method outlined. In contrast to all hitherto reported investigations [14–17, 34] we arrive at the conclusion that the conventional Curie transitions of EuS and EuO are first order with nearly the same discontinuity of the normalized order parameter of $\Delta m = 0.11 \pm 0.01$. In [15], for instance, data points with $m < 0.11$ are missing in the log–log plot of the spontaneous magnetization of EuO as a function of the reduced temperature.

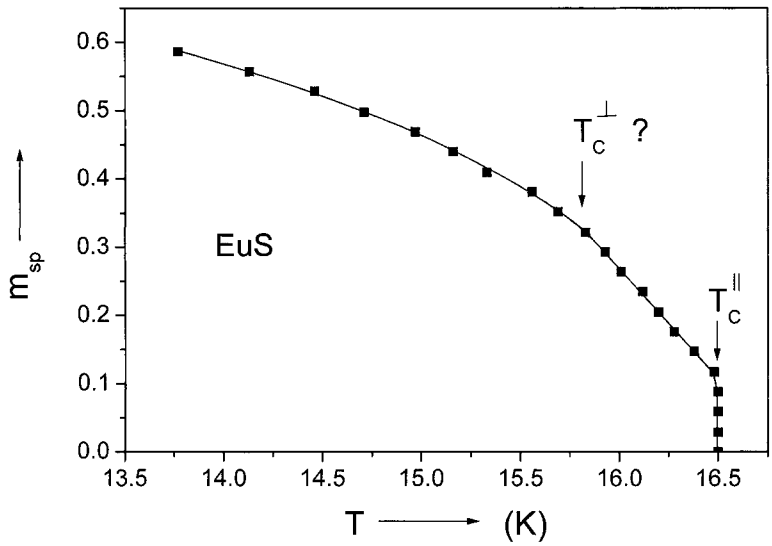

Figure 10. Normalized spontaneous magnetization, $m_{sp}(T)$, of EuS obtained from extrapolations $\chi^{\perp} \to 3$ in figure 9. A discontinuous rise at $T_C^{\parallel} = 16.5$ K classifies the conventional Curie transition as first order. The obtuse kink at $T_C^{\perp} = 15.7$ K can be interpreted as the Curie temperature of O_4.

A discontinuity of the order of 0.1 is hardly detected with neutron scattering. Considering that the scattering intensities are proportional to m^2 a discontinuity of $\Delta m = 0.1$ only gives rise to a 1% effect in the scattering intensities. Earlier neutron scattering studies on EuS and EuO were limited to $m > 0.25$ because of such intensity problems [14]. Also the NMR experiment on EuS was not conducted to $m < 0.25$ and therefore failed to observe the first-order character of $T_C^{\parallel}$ [34].

We should note that we are dealing with—as in the case of MnS_2 [20]—a particular first-order type transition caused by strong fourth-order interactions. At this transition the linear susceptibility diverges with the Heisenberg critical exponent of $\gamma \sim 1.4$ (see figure 9). Moreover, no indications for latent heat [35–40] or lattice distortion [41] are given.

The spontaneous magnetization curve given in figure 10 consists of three sections according to the three different groups of ac susceptibility curves in figure 9: a discontinuous rise at $T_C^{\parallel}$, a nearly linear behaviour in the range 15.8 K $< T < T_C^{\parallel}$ and a much weaker temperature dependence for $T < 15.8$ K. Whether the obtuse kink at $T = 15.8$ K can be identified with the Curie temperature $T_C^{\perp}$ of O_4 requires more detailed investigations. It should be noted that this anomaly is absent in the $Eu_xSr_{1-x}S$ samples with $x < 0.87$, for which fourth-order interactions are antiferromagnetic [22]. In fact, an antiferromagnetic O_4 should not contribute to the field parallel magnetization except for a reduced saturation magnetic moment.

3. Conclusions

This experimental investigation was restricted to cubic materials with pure spin magnetism. In the selected materials the magnetic interactions can be assumed to be isotropic and dominated by quantum mechanical exchange processes. Using magnetization measurements and neutron scattering we obtained evidence that in all materials a second ordering structure to

be attributed to fourth-order exchange interactions exists. The character of this ordering process (ferromagnetic or antiferromagnetic) always conforms to the sign of the fourth-order interaction sum evaluated from measurements of the cubic susceptibility χ_3. For instance, for the antiferromagnetic metals GdS and GdAg, χ_3 is negative (the paramagnetic isotherms increase stronger than linearly with field) meaning that fourth-order interactions are ferromagnetic. Consistent with this, macroscopic susceptibility measurements indicate that the associated ordering structure is ferromagnetic. In both antiferromagnets it is observed that χ_3 diverges (with a negative amplitude) at the critical temperature of O_4. This is taken as evidence that the transition is driven by fourth-order interactions.

It should be noted that existence of a true long range magnetic order associated with O_4 has not been proven for all the materials listed in table 1 using the microscopic method of neutron scattering. Normally, the saturation moment of O_4 is only weak and often below the sensitivity limits of conventional neutron scattering. The only exception known so far is GdMg with an ordered saturation moment of O_4 as large as $\sim 5\ \mu_B$ [31]. For EuTe, for instance, a molecular field analysis of the low-temperature magnetization curve revealed a ratio of fourth-order to second-order molecular field constants of $0.5T/8T = 0.06$ [2, 25]. Assuming that the ordered moments of antiferromagnetic O_2 and ferromagnetic O_4 scale with this ratio, an ordered ferromagnetic moment of only $0.4\ \mu_B$ can be estimated for O_4. For those materials for which second-order and fourth-order interactions are both ferromagnetic (EuS, EuO) or both antiferromagnetic ($Eu_{0.75}Sr_{0.25}Te$) the two order parameters give rise to the same set of Bragg lines and cannot be distinguished without applying a magnetic field. While for the antiferromagnet $Eu_{0.75}Sr_{0.25}S$ the two characteristic critical field curves can easily be detected with magnetization and neutron scattering measurements [5], a quite normal magnetic behaviour is observed for EuS and EuO except in the critical temperature range. Also for the ordered antiferromagnetic moment of O_4 in $Eu_xSr_{1-x}S$ with $x < 0.87$ our magnetization measurements indicate a value of only $0.1 \ldots 0.2\ \mu_B$. Such small moments are difficult to detect with neutron scattering without polarization analysis.

In those materials in which we evaluated the strengths of the fourth-order interactions quantitatively [3–6] it was observed that they compare with the strengths of the second-order Heisenberg interactions. One observation which demonstrates this is the fact that the critical temperatures of the two associated order parameters, O_2 and O_4, are very similar or even identical.

Comparison with classical electrodynamics seems to be revealing. The leading terms in the series expansion of the classical electrodynamic interaction according to increasing powers of the reciprocal distance are magnetic dipole–dipole and electric quadrupole–quadrupole interaction. Both interaction types can lead to well distinguished ordering processes which are described by a dipolar and a quadrupolar order parameter, respectively [42, 43]. A number of magnetic materials such as TmZn [44], CeAg [45], $DyVO_4$ [46] $TbVO_4$ [47] and TmTe [48] are known to show classical behaviour with weakly coupled dipolar and quadrupolar order parameters. In these materials the two order parameters have well separated transition temperatures.

In quantum mechanics the leading interaction processes are bilinear (Heisenberg) exchange interaction and fourth-order exchange interaction. Since exchange interactions are much stronger than dipolar interactions, the associated transition temperatures are also much higher. Apparently, also in quantum mechanical systems the different terms in the series expansion of the exchange interaction lead to different ordering processes and generate distinguished order parameters. In contrast to the classical quadrupole–quadrupole interaction it is intuitively not clear what the order parameter induced by fourth-order interactions is. Our investigations give a strong indication that fourth-order interactions break the rotational

symmetry of the collinearly ordered spin system. In this way biaxial ordering structures are also possible in cubic crystals with pure spin moments. For a ferromagnet the conventional order parameter O_2 is evidently given by the expectation value $\langle S_z \rangle$. O_4 can therefore be identified with the expectation value of the transverse spin component $\langle S_x \rangle$. As a consequence, existence of O_2 seems to be a necessary condition for ordering of O_4, which means that the transition temperature of O_4 will never be larger than the transition temperature of O_2. This is in contrast to the classical case for which the quadrupolar ordering temperature can be larger as well as smaller than the dipolar ordering temperature. For the materials selected here, quadrupolar interactions can be assumed to be negligibly small.

Our ac susceptibility measurements in the critical temperature range of EuS and EuO are in keeping with the mean field prediction of a discontinuous rise of the order parameter at the Curie temperature [7–10]. This was not realized in many experimental studies before [14–17]. As is well known, considerable experimental as well as methodical ambiguities exist in the evaluation of the critical behaviour of the order parameter. This also applies for our ac susceptibility measurements. However, for other experimental methods such as NMR and neutron scattering these problems are by no means less. In particular, these two methods suffer from considerable intensity problems and line broadening effects near T_C. Ac susceptibility measurements seem to be very sensitive in the critical temperature range where the magnetization changes vary rapidly as a function of temperature and field. In a forthcoming publication [22] we will show that EuS and EuO are not exceptions but that in almost all materials the phase transition either of O_2 or O_4 is first order.

It should be recalled that depending on which quantity is discontinuous, as well as the causative mechanism [49], there are different types of first-order transitions. A classification must include criteria such as whether or not the phase transition is accompanied by a lattice distortion, latent heat or hysteresis. For the first-order type magnetic phase transitions discussed here, with a discontinuity only of the order parameter, those effects seem to be negligibly small.

In conclusion, the situation in the critical temperature range of EuS and EuO is too complicated to allow observation of the critical behaviour for isotropic three-dimensional materials with half-integral spins. The reasons for this are twofold: first, the phase transition of O_2 appears to be first order and, second, the phase transition of O_4 seems to be very near to the Curie temperature of O_2. Therefore, other materials with well separated transition temperatures for O_2 and O_4 must be chosen in order to evaluate the intrinsic critical behaviour at the two-phase transitions. This is realized in GdMg with also a half-integral spin of $S = 7/2$. Interestingly, the Curie transition of O_2 is second order in GdMg and exhibits mean-field critical behaviour [1].

Acknowledgments

We thank Th Brückel for helpful discussions and critical comments on the manuscript. We are indebted to W Schnelle for performing specific heat measurements on GdAg. The technical assistance of B Olefs is gratefully acknowledged.

References

[1] Köbler U, Mueller R M, Schnelle W and Fischer K 1998 *J. Magn. Magn. Mater.* **188** 333
[2] Mueller R M, Köbler U and Fischer K 1999 *Eur. Phys. J.* B **8** 207
[3] Köbler U, Mueller R, Smardz L, Maier D, Fischer K, Olefs B and Zinn W 1996 *Z. Phys.* B **100** 497
[4] Müller-Hartmann E, Köbler U and Smardz L 1997 *J. Magn. Magn. Mater.* **173** 133
[5] Köbler U, Hoser A, Graf H A, Fernandez-Diaz M-T, Fischer K and Brückel Th 1999 *Eur. Phys. J.* B **8** 217

[6] Köbler U and Fischer K 2001 *J. Phys.: Condens. Matter* **13** 123
[7] Rodbell D S, Jacobs I S, Owen J and Harris E A 1963 *Phys. Rev. Lett.* **11** 10
[8] Matveev V M and Nagaev E L 1972 *Sov. Phys.–Solid State* **14** 408
[9] Adler J and Oitmaa J 1979 *J. Phys. C: Solid State Phys.* **12** 575
[10] Girardeau M D and Popovic-Bozic M 1977 *J. Phys. C: Solid State Phys.* **10** 4373
[11] Köbler U, Hoser A, Kawakami W, Chatterji T and Rebizant J 1999 *J. Magn. Magn. Mater.* **205** 343
[12] Bloch F 1930 *Z. Phys.* **61** 206
[13] Dyson F J 1956 *Phys. Rev.* **102** 1230
[14] Als-Nielsen J, Dietrich O W and Passell L 1976 *Phys. Rev.* B **14** 4908
[15] Menyuk N, Dwight K and Reed T B 1971 *Phys. Rev.* B **3** 1689
[16] Berkner D D 1975 *Phys. Lett.* A **54** 396
[17] *Landolt-Börnstein* 1982 vol III 12, pt c (Berlin: Springer) pp 173–4
[18] Westrum E F Jr and Gronvold F 1970 *J. Chem. Phys.* **52** 3820
[19] Scheer E, Wosnitza J, v Löhneysen H, Kürsch R, Lang M and Steglich F 1992 *J. Magn. Magn. Mater.* **104–7** 175
[20] Chattopadhyay T, v Schnering H G and Graf H A 1984 *Solid State Commun.* **50** 865
[21] Lin M S and Hacker H Jr 1968 *Solid State Commun.* **6** 687
[22] Köbler U, Mueller R M, Hoser A, Brown P J, Chatterji T, Fischer K, Rebizant J and Wallrafen F *Eur. Phys. J.* B to appear
[23] Köbler U, Hupfeld D, Schnelle W, Mattenberger K and Brückel Th 1999 *J. Magn. Magn. Mater.* **205** 90
[24] Köbler U, Schweizer J, Chieux P, Lorenz Th, Büchner B, Schnelle W, Deloie F and Zinn W 1997 *J. Magn. Magn. Mater.* **170** 110
[25] Köbler U, Apfelstedt I, Fischer K, Zinn W, Scheer E, Wosnitza J, v Löhneysen H and Brückel T 1993 *Z. Phys.* B **92** 475
[26] Nowotny R M and Binder K 1989 *Z. Phys.* B **77** 287
[27] Kiessler G, Gebhardt E and Steeb S 1972 *J. Less-Common Met.* **26** 293
[28] Schnelle W 1999 private communication
[29] Borovik-Romanov A S, Bazhan A N and Kreines N M 1973 *Sov. Phys.–JETP* **37** 695
[30] Aleonard R, Morin P, Pierre J and Schmitt D 1975 *Solid State Commun.* **17** 599
[31] Morin P, Pierre J, Schmitt D and Givord D 1978 *Phys. Lett.* A **65** 156
[32] Buschow K H J and Schinkel C J 1976 *Solid State Commun.* **18** 609
[33] Pierre J, de Combarieu A and Lagnier R 1979 *J. Phys. F: Met. Phys.* **9** 1271
[34] Heller P and Benedek G 1965 *Phys. Rev. Lett.* **14** 71
[35] Kornblit A and Ahlers G 1975 *Phys. Rev.* B **11** 2678
[36] Kornblit A, Ahlers G and Buehler E 1978 *Phys. Rev.* B **17** 282
[37] Wosnitza J and v Löhneysen H 1989 *Europhys. Lett.* **10** 381
[38] Scheer E, Wosnitza J and v Löhneysen H 1991 *Z. Phys.* B **85** 79
[39] Lederman F L, Salamon M B and Shacklette L W 1974 *Phys. Rev.* B **9** 2981
[40] Stroka B, Wosnitza J, Scheer E, v Löhneysen H, Park W and Fischer K 1992 *Z. Phys.* B **89**
[41] Levy F 1969 *Phys. Kondens. Mater.* **10** 71
[42] Morin P and Schmitt D 1983 *Phys. Rev.* B **27** 4412
[43] Morin P and Schmitt D 1990 *Ferromagnetic Materials* vol 5 ed K H J Buschow and E P Wohlfarth (Amsterdam: Elsevier)
[44] Morin P, Rouchy J and Schmitt D 1978 *Phys. Rev.* B **17** 3684
[45] Ushizaka H, Murayama S, Miyako Y and Tazuke Y 1984 *J. Phys. Soc. Japan* **53** 1136
[46] Cooke A H, Martin D M and Wells M R 1971 *Solid State Commun.* **9** 519
[47] Sayetat F 1972 *Solid State Commun.* **10** 879
[48] Matsumura T, Nakamura S, Goto T, Amitsuka H, Matsuhira K, Sakakibara T and Suzuki T 1998 *J. Phys. Soc. Japan* **67** 612
[49] Bean C P and Rodbell D S 1962 *Phys. Rev.* **126** 104